appropriate background corrections were carried out with the computer program SpectraCalc (Galactic Industries).

ESR Spectra. ESR spectra were recorded at 9.52 GHz on a Bruker Model ER200D spectrometer equipped with an ESP1620 data system. Samples were thoroughly degassed under vacuum and flame sealed in quartz tubes.

Emission Spectra. Near-IR emission spectra of the cation radicals were determined with a SPEX 212 Fluorimeter (Spex Industries) modified to accept a high-sensitivity germanium detector (North Coast Model EO-817L, useful wavelength range ≈750–1750 nm). Spectra were corrected for detector and optical system response by using curves determined with a NBS traceable calibrated tungsten lamp (Optronics Laboratories). Signal to noise was improved via lock-in detection (Stanford Instruments with the chopper located at the entrace slit of the emission monochrometer). Scattered light was removed by use of either short wave pass or narrow band pass interference filters (Corion Corp.) placed between the excitation monochrometer and the sample and by use of long wave pass interference filters (Corion Corp.) placed between the sample and the emission monochrometer. Background scans of both as prepared and activated zeolite samples showed no detectable emission in this wavelength region.

Acknowledgment. We thank A. Pittman, D. Sanderson, and P. Hollins for able technical assistance.

Preparation and Spectroscopic Characterization of Polarons and Bipolarons of Thiophene Oligomers within the Channels of Pentasil Zeolites: The Evolution of Organic Radical Ions into Conducting Polymers†

Jonathan V. Caspar,* V. Ramamurthy,* and David R. Corbin

Contribution from E. I. du Pont de Nemours & Company, Central Research and Development Department, Experimental Station, P.O. Box 80328, Wilmington, Delaware 19880-0328.
Received July 9, 1990

Abstract: Pentasil zeolites such as ZSM-5 and Na-β can be used as supporting matrices in which short-chain oligomers of polythiophene can be prepared, oxidatively doped to the conducting state, stabilized, and finally spectroscopically characterized. For the first time the evolution of the electronic structure of doped polythiophene from monomer to polymer has been observed directly for chain lengths between two and nine. Plots of the electronic absorption band energies for the polaron and bipolaron are found to be linear functions of inverse chain length. These results are extrapolated to infinite chain length to predict the positions of heretofore unobserved electronic transitions of bulk polythiophene. These extrapolations suggest that the lowest energy polaron and bipolaron levels of doped polythiophene are remarkably close in energy, implying that transient formation of polarons from bipolarons is energetically feasible and that this process could play a role in interchain charge hopping in this material.

Introduction

We recently reported that following activation at modestly high temperatures certain types of pentasil zeolites such as ZSM-5 and Na-β can effect the room temperature oxidation of included α,ω-diphenyl polyenes to yield stabilized cation radicals of the parent olefins. These cation radicals, which are protected within the zeolite channels, persist for months even in the presence of air and water and can be characterized via conventional spectroscopic techniques.[1] While we were unable to determine the precise nature of the zeolite-based oxidant, we were able to demonstrate that its effective redox potential is near 1.6 ± 0.1 eV vs SCE and that the presence of aluminum in the zeolite framework is essential to observe oxidation. Precedent for this type of one-electron-oxidation of guests in zeolites also comes from the work of both Ozin et al., who observed oxidation of metallocenes in zeolite Y,[2] and Bauld et al., who have inferred cation radical formation in Diels–Alder reactions catalyzed by zeolites.[3,4]

These observations suggested to us a simple method by which isolated conducting polymer strands and/or oligomers might be prepared and doped to their conducting state within the confines of a zeolite channel. It is well-known that one-electron oxidation of thiophene leads to rapid formation of polythiophene resulting from linking monomers in the α-position. The neutral polymer can be doped electrochemically to yield electronically conducting polythiophene.[5]

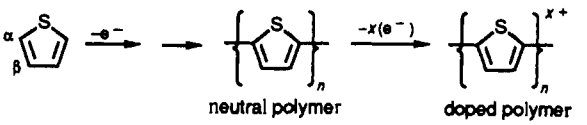

Given the oxidation potentials of oligomeric thiophenes (<1.3 eV vs SCE for $n \geq 2$), we expected that the zeolite-based oxidant would be capable of oxidizing them, leading to oligomerization/polymerization within the zeolite interior as outlined above. In this paper we demonstrate that this oligomerization does occur and that the zeolite-based oxidant can be used to prepare and stabilize cationically doped thiophene oligomers which can then be characterized by conventional spectroscopic techniques. The zeolite encapsulation has the added advantage of yielding oligomers that are well-isolated from one another so that effects due to interchain contacts are eliminated.

The evolution of electronic structure of organic conducting polymers with chain length remains an intriguing unresolved problem. In principle the problem is easily addressed simply by determining the spectroscopic properties of short-chain oligomers

† Part of the series Modification of Photochemical Reactivity by Zeolites.

(1) Ramamurthy, V.; Caspar, J. V.; Corbin, D. R. *J. Am. Chem. Soc.*, preceding paper in this issue.
(2) Ozin, G. A.; Godhber, J. *J. Phys. Chem.* **1989**, *93*, 878–893.
(3) Bauld, N. L. *Tetrahedron* **1989**, *45*, 5307–5363.
(4) Ghosh, S.; Bauld, N. L. *J. Catal.* **1985**, *95*, 300–304.
(5) Skotheim, T. A. *Handbook of Conducting Polymers*; Marcel Dekker, Inc.: New York, 1986; Vols. 1 and 2.

0002-7863/91/1513-600$02.50/0

of known length and relating the observed parameters to theoretical models. However in practice this proves difficult for anything other than the undoped neutral oligomers. In general the difficulty lies in the fact that the doped short-chain oligomers are inherently reactive species. In the particular case of polythiophene, the oxidatively doped oligomers are unstable with respect to further oligomerization; the polymers are prepared by one-electron oxidation. To further complicate matters, in the case of cationically doped polythiophene two charged species are formed (polarons and bipolarons, see below) which are expected to have discrete spectroscopic signatures. The difficulty which arises then, is how to prepare oligomers of known chain length, oxidatively dope them to a controlled level (either polaron or bipolaron), and stabilize the resulting materials so they can be investigated spectroscopically. In this paper we will demonstrate how this can be accomplished within the interior channels of zeolites. The results of these experiments will allow us to map out the evolution of electronic structure of cationically doped polythiophene for oligomers with chain lengths in the size regime where molecular properties are evolving into bulk polymer properties ($2 \leq n \leq 9$), enabling us to address the question of how long an oligomer chain must be before it is properly considered to be a polymer in the electronic sense. While this work was in progress the first reported steady-state absorption spectrum of the polaron of a thiophene oligomer (α-sexithiophene, $n = 6$) was reported. Lower oligomers were investigated and found to react too rapidly for their spectra to be determined. Determination of the electronic spectrum of the dication (bipolaron) of α-sexithiophene was precluded by the insolubility of the doubly oxidized product.[6]

Before discussing our approach to the stabilization of polarons and bipolarons of short-chain thiophene oligomers it will be necessary to briefly summarize the properties of the zeolite hosts we will employ as supporting matrices. Zeolites are a large class of crystalline microporous solids with the general formulation $M_x[(AlO_2)_x(SiO_2)_y]\cdot n(H_2O)$ which find wide application as sorbents, ion exchangers, catalysts, and catalyst supports. Their structure is based on a three-dimensional network of AlO_4^{5-} and SiO_4^{4-} tetrahedra which are linked to each other via doubly bridging oxygen atoms.[7,8] As each aluminum atom incorporated into the network leads to the presence of one excess negative charge, charge compensating cations (M^+) must be introduced into the structure. These cations are not covalently bound to the zeolite framework and are readily exchanged. In this paper we will employ primarily the zeolites Na-ZSM-5 (the Na^+ exchanged form of the zeolite ZSM-5) and Na-β. X-ray diffraction structural analyses of ZSM-5 reveal that it possesses two types of pore systems.[9] One pore type is sinusoidal with a nearly circular cross section of about 5.5 Å. The other is straight with an elliptical cross section of 5.2 × 5.5 Å (Figure 1). In general, Na-ZSM-5 zeolite (Si/Al = 22; $x = 4.2$; x is defined as in the generic formula above) was used for most of the work reported here; however, ZSM-5 exchanged with other cations (Li, K, Cs, Tl) and with varying Si/Al ratios ($22 < Si/Al < 550$) were also examined. In addition we have also employed the less sterically demanding zeolite Na-β which possesses two sets of perpendicular channels with dimensions significantly larger than those in ZSM-5 (one circular with a 5.6-Å diameter and one elliptical with dimensions 6.0 × 7.3 Å). The channels intersect to form a three-dimensional array of cages with diameters of 12–13 Å.[10–12]

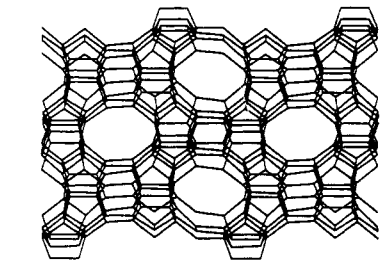

(A)

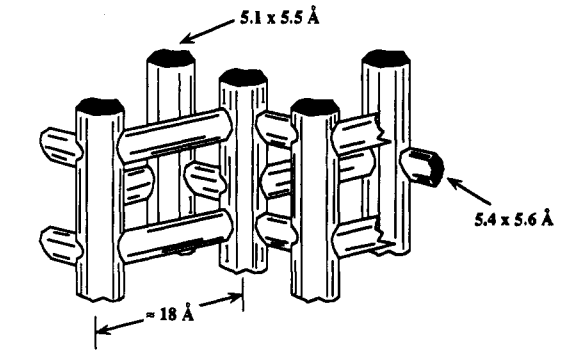

(B)

Figure 1. (A) The structure of ZSM-5 showing the view along the direction of the straight channel. Vertices represent Si or Al atoms and bonds between vertices represent doubly bridging O atoms. (B) Schematic picture of the channel structure of ZSM-5 showing the straight and zigzag channel systems.

We are not the first to attempt the preparation of conducting polymers within the protected confines of host lattices such as clays, zeolites, or other inorganic matrices. The earliest reports are of polymerization/oligomerization in clays with formation of poly-*p*-phenylene from benzene[13] and what was probably polythiophene from thiophene.[14] The first detailed reports of polymerization of thiophene and benzene in the interlayers of clays were due to Soma et al.,[15–18] who used clays exchanged with transition-metal cations (Cu^{2+}, Fe^{3+}) to oxidize included thiophene leading to formation of polythiophene. A variety of spectroscopic techniques (resonance Raman, EPR, IR, UV–vis) suggested the formation of doped conducting polymer, although the chain lengths and conductivity were not determined. Similar experiments have also been reported for polymerization of pyrrole within the layered host FeOCl[19,20] and the three-dimensional coordination polymer host $[(Me_3Sn)_3Fe(CN)_6]_\infty$,[21] in both of these cases yielding doped polypyrrole composites. The first report of formation of conducting polymers in zeolites instead of clays was made by Chao, who observed polymerization of pyrrole in Fe^{3+} and Cu^{2+} exchanged zeolite Y.[22] While our work was in progress, Bein et al. also reported similar experiments using transition-metal-exchanged zeolites (mordenite and zeolite Y exchanged with Cu^{2+}, Fe^{3+}) as

(6) Fichou, D.; Horowitz, G.; Xu, B.; Garnier, F. *Springer Ser. Solid-State Sci.* **1989**, *91*, 386–393.
(7) Breck, D. W. *Zeolite Molecular Sieves*; Robert E. Krieger Publishing Co.: Malabar, FL, 1974.
(8) Dyer, A. *An Introduction To Zeolite Molecular Sieves*; John-Wiley and Sons: New York, 1988.
(9) Meier, W. M.; Olsen, D. H. *Atlas of Zeolite Structure Types*; Butterworths: London, 1988.
(10) Newsam, J. M.; Treacy, M. M. J.; Koetsier, W. T.; de Gruyter, C. B. *Proc. R. Soc. London A* **1988**, *420*, 375–405.
(11) Higgins, J. B.; LaPierre, R. B.; Schlenker, J. L.; Rohrman, A. C.; Wood, J. D.; Kerr, G. T.; Rohrbaugh, W. J. *Zeolites* **1988**, *8*, 446.
(12) Benslama, R.; Fraissard, J.; Albizane, A.; Fajula, F.; Figueras, F. *Zeolites* **1988**, *8*, 196–198.
(13) Pinnavaia, T. J.; Hall, P. L.; Cady, S. S.; Mortland, M. M. *J. Phys. Chem.* **1974**, *78*, 994–999.
(14) Cloos, P.; Poel, D. V.; Camerlynck, J. P. *Nature* **1973**, *243*, 54–55.
(15) Soma, Y.; Soma, M.; Harada, I. *Chem. Phys. Lett.* **1983**, *99*, 153–156.
(16) Soma, Y.; Soma, M.; Harada, I. *J. Phys. Chem.* **1984**, *88*, 3034–3038.
(17) Soma, Y.; Soma, M.; Harada, I. *J. Phys. Chem.* **1985**, *89*, 738–742.
(18) Soma, Y.; Soma, M.; Furukawa, Y.; Harada, I. *Clays Clay Miner.* **1987**, *35*, 53–59.
(19) Kanatzidis, M. G.; Hubbard, M.; Tonge, L. M.; Marks, T. J.; Marcy, H. O.; Kannewurf, C. R. *Synth. Met.* **1989**, *28*, C89–C95.
(20) Kanatzidis, K. G.; Tonge, L. M.; Marks, T. J.; Marcy, H. O.; Kannewurf, C. R. *J. Am. Chem. Soc.* **1987**, *109*, 3797.
(21) Brandt, P.; Fischer, R. D.; Martinez, E. S.; Calleja, R. D. *Angew. Chem., Int. Ed. Engl.* **1989**, *28*, 1265–1266.
(22) Chao, T. H.; Erf, H. A. *J. Catal.* **1986**, *100*, 492–499.

hosts to facilitate the polymerization of pyrrole, aniline, and thiophene within the zeolites' interiors.[23-27] Characterization of the resulting zeolite encapsulated polymers rests primarily upon infrared, Raman, and limited visible absorption spectra. As in the earlier work of Soma, chain lengths of the resulting polymers were not determined. Bein determined that the zeolite/conducting polymer composites were nonconducting, suggesting that the polymers did not form unbroken continuous strands traversing entire zeolite crystallites. Chemical oxidation of furans and thiophenes in Cu^{2+} exchanged ZSM-5 and zeolite Y to yield cation radicals characterized by EPR has also been reported very recently.[28] Finally, catalytic formation of polyacetylene on the exterior surfaces of transition-metal-exchanged small-pore zeolites has also been demonstrated with resonance Raman spectroscopy.[29]

In this paper, our approach will be to oligomerize the preformed neutral thiophene oligomers (**2**, **3**, **4**, **6**) and not thiophene itself. Oligomers **2**–**4** are known to be polymerized upon oxidation in

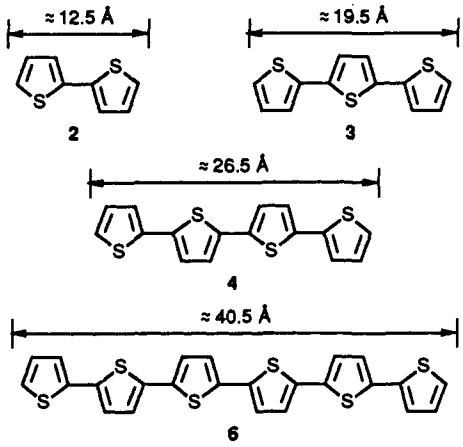

the same manner as thiophene, in some cases leading to bulk polythiophene with improved electronic conductivity.[30,31] There are several reasons for choosing to start with preformed oligomers. First, we previously demonstrated that the effective redox potential of the zeolite-based oxidation site is near 1.6 eV vs SCE,[1] which is not sufficiently positive to oxidize thiophene itself (a prediction which we confirmed experimentally; thiophene is not oxidized by the zeolites which we employ). However the oxidation potentials of thiophene oligomers decrease with increasing chain length, with the result that **2**, **3**, **4**, and **6** all have potentials less positive than 1.6 eV and should be oxidized within the zeolite channels. A second reason for using oligomers is that for chain lengths longer than two, molecular models suggest only the straight channel in ZSM-5 is sterically accessible (note the lengths of the oligomers as estimated from CPK models), which should lead to formation of well-isolated polymer chains with an enforced linear geometry. Oligomerization reactions within the zeolite will be forced to proceed only at the terminal (α) positions and not at the β positions. Polymerization at the β position is known in the case of bulk polythiophene to lead to polymer with inferior conductivity properties.[32-34] Thiophene monomer is small enough to enter either the straight or zigzag channels in ZSM-5 which could result both in cross-linking between chains and in a greater variety of chain geometries, making spectroscopic assignments more difficult.

Another advantage of the oligomeric precursors is the resulting ability to establish chain lengths by comparing products obtained from different precursors with the knowledge that if the same product is formed from two different precursors then its chain length must be a common multiple of those of the precursors (i.e. octamer can be formed from **2** and **4**, but not from **3** or **6**).

Finally, in the channels of the zeolite supports which we will employ, it is likely that the longer oligomers will diffuse more slowly than monomer which should lead to slower polymerization rates for the oligomeric precursors. As we are particularly interested in observing short-chain oligomers ($n \lesssim 10$), this decrease in reaction rate represents a significant advantage.

Experimental Section

Reagents. Thiophene and α-terthiophene (**3**) were used as received (Aldrich). 2,2'-Bithiophene (**2**, Aldrich) was chromatographed on silica gel in hexane and stored under nitrogen prior to use. α-Quaterthiophene (**4**),[35] α-sexithiophene (**6**),[35] 5-methylterthiophene,[36] 5,5'-dimethylterthiophene,[36] and 5,5'-dimethylquaterthiophene[35] were prepared by literature methods.

Preparation of Zeolites. Zeolite samples ZSM-5 and Na-β were prepared as described below following literature procedures and were characterized by ICP elemental analysis and powder X-ray diffraction.

ZSM-5: Samples of Na-TPA-ZSM-5 with Si/Al varying from 20 to 550 were prepared by a slight modification of Rollman and Volyocsik's procedure.[37] Samples were calcined in flowing air at 60 °C/h to 550 °C and then held at 550 °C for 10 h to give Na-ZSM-5. The samples were then exchanged by conventional methods to give Li-ZSM-5, K-ZSM-5, Cs-ZSM-5, and Tl-ZSM-5. These samples were stored under ambient conditions.

Na-β: Samples of Na-β were prepared by literature methods;[38] calcined in flowing air at 60 °C/h to 550 °C, and then held at 550 °C for 10 h to give Na-β.

Activation of Zeolites. In general, ca. 250 mg of zeolite was placed in a silica crucible and heated at 500 °C for about 12 h. The freshly activated zeolites were rapidly cooled in air to ca. 50 °C and added to solutions of the thiophene of interest. The activated zeolites were used immediately after activation.

Preparation of Complexes. Weighed amounts of thiophene oligomers and activated zeolite (as above) were stirred together in 20 mL of trimethylpentane for about 2 h. In a typical preparation, 250 mg of the zeolite and 5 mg of the α-terthiophene were stirred in 20 mL of the solvent. During this process the zeolite complex developed color which varied depending upon the chain length of the oligomer. The colored zeolite complexes were collected by filtration, washed with hexane several times to remove any material adsorbed on the external surface of the crystallites, dried under nitrogen, and finally thoroughly degassed (10^{-4} mm) in either Pyrex or quartz cells fitted with Teflon stopcocks. These cells were used for recording absorption, emission, and EPR spectra.

UV-vis-NIR Diffuse Reflectance Spectra. Diffuse reflectance spectra of the above zeolite solid samples were measured in 2 mm path length quartz cells on a Varian 2400 spectrometer equipped with either an integrating sphere (Varian) or a "Praying Mantis" all reflective light collection system (Harrick Scientific) in both cases with barium sulfate (Kodak, White Reflectance Standard) as the reference. Sample packing densities were not determined nor were they specifically controlled. Spectra were recorded between 220 and 2000 nm. For comparison, spectra of the activated zeolites were also recorded. Reflectance data were recorded digitally and appropriate background corrections and transformation of the data to Kubelka-Munk form were carried out with use of the computer program SpectraCalc (Galactic Industries, Version 2.2).

EPR Spectra. X-band EPR spectra were recorded at 9.5 GHz on a Bruker Model ER200D spectrometer equipped with an ESP-1620 data system. Samples were thoroughly degassed under vacuum and flame sealed in quartz tubes. Spectra determined at temperatures above ambient were recorded on a Bruker Model ER-420 spectrometer equipped with a Bruker Model B-VT-1000 variable-temperature controller.

(23) Enzel, P.; Bein, T. *J. Chem. Soc., Chem. Commun.* **1989**, 1326-1327.
(24) Bein, T.; Enzel, P. *Synth. Met.* **1989**, *29*, 163-168.
(25) Enzel, P.; Bein, T. *J. Phys. Chem.* **1989**, *93*, 6270-6272.
(26) Bein, T.; Enzel, P.; Beuneu, F.; Zuppiroli, L. *Adv. Chem.* **1990**, *226*, 433-449.
(27) Bein, T.; Enzel, P. *Mol. Cryst. Liq. Cryst.* **1990**, *181*, 315-324.
(28) Hwang, B.; Chon, H. *Zeolites* **1990**, *10*, 101-104.
(29) Dutta, P. K.; Puri, M. *J. Catal.* **1988**, *111*, 453-456.
(30) Krische, B.; Hellberg, J.; Lilja, C. *J. Chem. Soc., Chem. Commun.* **1987**, 1476-1478.
(31) Mermilliod-Thevenin, N.; Bidan, G. *Mol. Cryst. Liq. Cryst.* **1985**, *118*, 227-233.
(32) Wu, C. R.; Nilsson, J. O.; Inganäs, O.; Salaneck, W. R.; Osterholm, J. E.; Brēdas, J. L. *Synth. Met.* **1987**, *21*, 197.
(33) Yamamoto, T.; Sanechika, K.; Yamamoto, A. *Chem. Lett.* **1981**, 1079.
(34) Salaneck, W. R.; Brēdas, J. L.; Wu, C. R.; Nilsson, J. O. *Synth. Met.* **1987**, *21*, 57.
(35) Kagan, J.; Arora, S. K. *Heterocycles* **1983**, *20*, 1937-1940.
(36) Arnason, J. T.; Philogene, B. J. R.; Berg, C.; Maceachern, A.; Kaminski, J.; Leitch, L. C.; Morand, P.; Lam, J. *Phytochemistry* **1986**, *25*, 1609-1611.
(37) Rollman, L. S.; Volyocsik, E. K. In *Inorganic Synthesis*; Wiley: New York, 1983; pp 61-68.
(38) Wadlinger, R. L.; Kerr, G. T.; Rosinski, E. J. US Patent 3,308,069, 1975, Example 7.

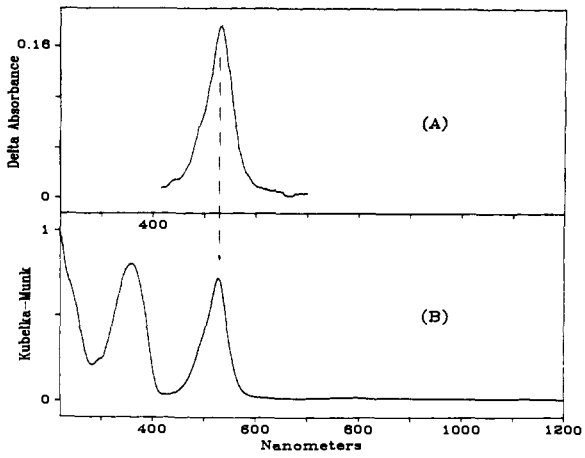

Figure 2. (A) The absorption spectrum of the cation radical of terthiophene, $3^{\bullet+}$, generated by flash photolysis as a solution transient. Data taken from ref 39. (B) Room temperature diffuse reflectance spectrum of terthiophene, **3**, included in Na-β showing the formation of the cation radical $3^{\bullet+}$.

Results and Discussion

Formation of Oligothiophene Cation Radicals (Polarons). In Figure 2, we present the results of our first experiment aimed at demonstrating that thiophene oligomers could be oxidized within the channels of pentasil zeolites. In this experiment, activated Na-β (chalk white) was loaded with terthiophene (**3**, pale yellow) as described in the Experimental Section to yield a deep red-purple complex whose diffuse reflectance spectrum is shown in the figure. In addition to the band at 350 nm which is due to neutral terthiophene, a new band is observed at 530 nm which is present in neither uncomplexed terthiophene nor activated zeolite. Similar spectroscopic changes were observed upon inclusion of terthiophene in Na-ZSM-5. Comparison with flash photolysis results where the terthiophene cation radical ($3^{\bullet+}$) is generated as a transient in solution via electron-transfer quenching (Figure 2)[39] shows excellent agreement with the diffuse reflectance spectrum. As expected for a simple cation radical, we can observe an EPR spectrum for $3^{\bullet+}$ although no hyperfine structure was resolved (Figure 3). This is consistent with our previous observation that in the case of α,ω-diphenylpolyene cation radicals generated inside Na-ZSM-5, only short-chain polyenes showed any detectable hyperfine structure, while longer chains gave broad unresolved lines. We believe that this is the result of hindered rotation of the larger guests within the zeolite channels.

The results obtained for terthiophene included in Na-β and Na-ZSM-5 are not unique. We have observed the same types of one-electron-oxidation reactions for bithiophene (**2**) and quaterthiophene (**4**) included in either ZSM-5 or Na-β. The observed peak position for $2^{\bullet+}$ (420 nm) is in good agreement with the value determined recently by Scaiano via flash photolysis.[40] As shown in Figure 4, the absorption bands due to the neutral oligomers and the longer wavelength bands due to the corresponding cation radicals shift to longer wavelengths with increasing chain lengths. We will return to this point below.

We have previously discussed the stabilization of cation radicals of α,ω-diphenyl polyenes in channel type zeolites and demonstrated that these radicals are not adsorbed on the external surfaces of the crystallites, but rather are located within the zeolite interior.[1] For the same reasons as those presented previously, we believe that this is the case for these samples as well. In particular, the stability of the cation radicals which exist only as reactive intermediates in solution is very much higher within the zeolite channels; we have stored samples of the terthiophene cation radicals for months without any significant degradation (except as noted below) even in the presence of air and water. The cation radicals cannot be extracted from the zeolite with polar solvents, further demonstrating their inaccessibility.

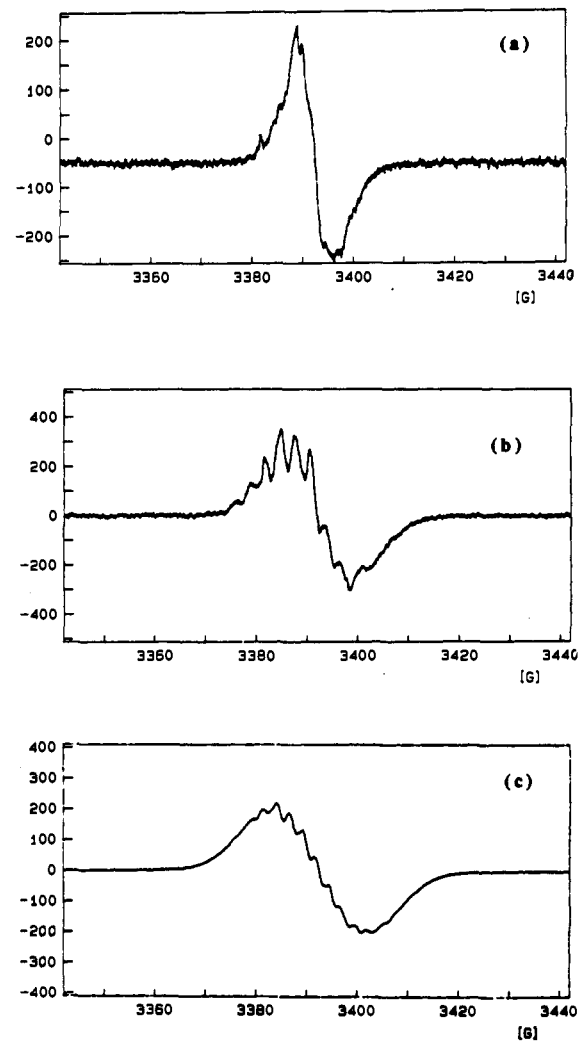

Figure 3. Room temperature EPR spectra of the cation radicals of (a) terthiophene (**3**), (b) methylterthiophene (**Me-3**), and (c) dimethylterthiophene (**Me_2-3**) included in Na-ZSM-5.

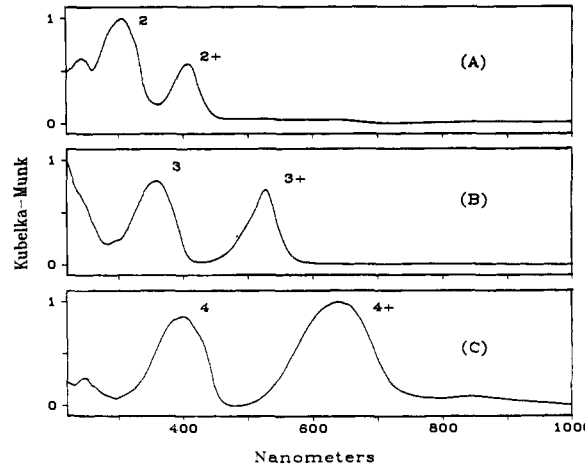

Figure 4. Room temperature diffuse reflectance spectra of (A) bithiophene (**2**), (B) terthiophene (**3**), and (C) quaterthiophene (**4**) included in Na-β. Transitions due to the neutrals and cation radicals are labeled.

An obvious and troubling aspect of this zeolite-based oxidation reaction is our inability to obtain any detailed information about the site of oxidation and the fate of the electron removed from the thiophene oligomers. Spectroscopically, we can find no new

(39) Scaiano, J. C.; Evans, C.; Arnason, J. T. *J. Photochem. Photobiol., B* **1989**, *3*, 411-418.
(40) Evans, C.; Scaiano, J. *J. Am. Chem. Soc.* **1990**, *112*, 2694-2701.

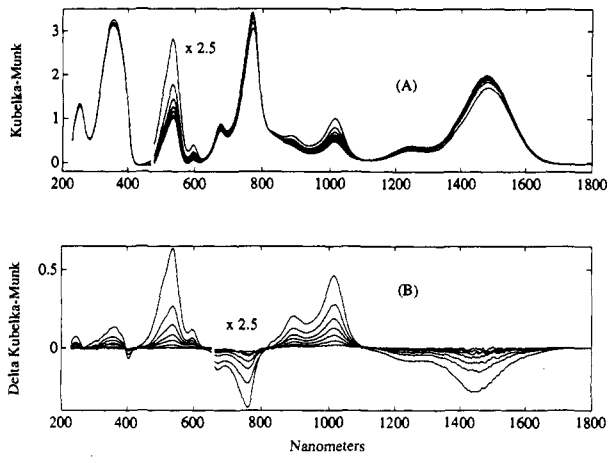

Figure 5. (A) Room temperature diffuse reflectance spectra of terthiophene included in ZSM-5 recorded at 2-h intervals. (B) Difference spectra for the series of scans in (A) presented as $R - R_\infty$ where R_∞ is the reflectance of the final scan. Peaks above zero are due to species whose concentrations are decreasing with reaction time and those below zero are increasing with reaction time. The reaction was followed to very near completion (at room temperature). An additional scan made after an additional 24 h of reaction was indistinguishable from the scan after 18 h.

optical absorption bands attributable to the reduced zeolite; however, the highly absorbing nature of the organic products could certainly obscure any weak zeolite transitions. In addition to the line at $g = 2.0028$ assigned to the terthiophene cation radical, EPR spectra do show a second very broad, weak line possibly associated with the reduced zeolite; however, we have not yet been able to unambiguously demonstrate this connection. Our general conclusion is simply that for the purpose of investigating the spectra of the thiophene oligomers, the fate of the removed electron is unimportant as long as the reaction is irreversible and it does not interfere spectroscopically, both of which appear to be the case.

As noted above, the cation radical of terthiophene is stable for extended periods within the channels of pentasil zeolites; however, it is not completely unreactive. On standing at room temperature or with mild heating (60–140 °C), we observe that new bands appear at longer wavelengths in the diffuse reflectance spectrum (see Figure 5). These bands are due not to decomposition of the cation radical but rather to further oligomerization to form hexamers and 9-mers. The complex appearance of the spectra in Figure 5 is the result of the presence of neutral terthiophene, terthiophene cation radical, terthiophene dication, α-sexithiophene dication, and α-nonathiophene dication. Before we turn to the detailed assignment of the spectra of these oligomers, we will first describe briefly our attempts to drive the oligomerization to longer chain length via controlled heating.

We have thus far described only the formation of short to medium chain length polythiophene oligomers within the channels of pentasil zeolites. In general, we have observed that at room temperature the rate of oligomerization drops dramatically as chain lengths increase. This is likely due to two factors: first, the decreased reactivity of the longer chain cation radicals decreases their oligomerization rate ($\mathbf{6}^{\bullet+}$ was recently reported to be stable enough in dilute solution that its electronic absorption spectrum could be determined), and second, the decreased rates of diffusion of the higher oligomers due both to increased size and charge. In practice, at room temperature we have not seen any significant formation of oligomers with chain lengths greater than 9 when starting with either **3** or **4**. An obvious way to circumvent this problem is to heat the samples in order to try and drive the reactions to form higher molecular weight polymer. In qualitative experiments, we have demonstrated that this approach does lead to materials with enhanced near-IR absorption consistent with the formation of longer chain polymer.[41] When the terminal

(41) Patil, A. O.; Heeger, A. J.; Wudl, F. *Chem. Rev.* **1988**, *88*, 183–200.

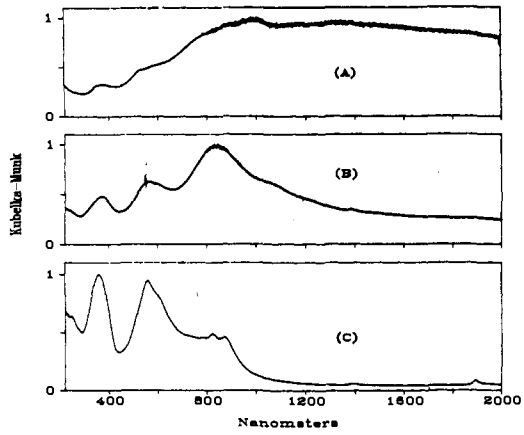

Figure 6. Room temperature diffuse reflectance spectra of **3** (A), **Me-3** (B), and $\mathbf{Me_2}$**-3** (C) included in Na-ZSM-5 after heating for 18 h at 140 °C. Note the absence of long-wavelength absorption for the methylated derivatives.

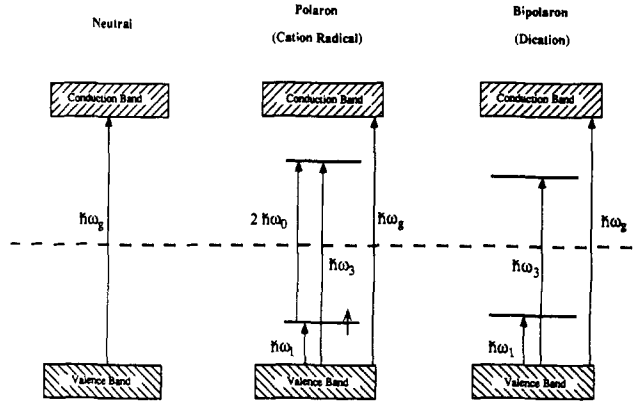

Figure 7. Simple band picture for the oxidative doping of polythiophene.

α-positions of the terthiophene are blocked with methyl groups, heating the initially formed cation radicals does not lead to increased near-IR absorption, consistent with blocking the site of the polymerization reaction (Figure 6, see below for further details of these experiments). However, at this time, we can offer no definitive evidence that the product resulting from heating terthiophene in ZSM-5 or Na-β is doped *high molecular weight* polymer.

Spectroscopy of Polythiophene and Oligothiophenes. The spectroscopic characterization of the charge carriers in doped conducting polymers in general and polythiophene in particular has received wide attention.[5,41–43] We will summarize here in only a very general way the models which have evolved and will only point out the predictions of theory as they apply to the complexes in which we will be interested. We recognize in advnace that these theoretical models neglect Coulomb interactions[44] and were explicitly developed for high molecular weight polymers where the number of π-orbitals per chain is large. As a result the detailed predictions will represent a considerable oversimplification for the short-chain oligomers in which we are interested. In particular, it is likely that these short-chain oligomers will retain discrete electronic transitions originating in levels within the conduction band which the band theory description does not explicitly recognize. However, we believe that the band picture offers significant insights into the trends we have observed and to first order offers a reasonable model for comparison with experiment.

Neutral polythiophene possesses two electronic bands, one filled and the other empty. The lowest optical transition is the band

(42) Brēdas, J. L.; Street, G. B. *Acc. Chem. Res.* **1985**, *18*, 309–315.
(43) Baughman, R. H.; Bredas, J. L.; Chance, R. R.; Elsenbaumer, R. L.; Shacklette, L. W. *Chem. Rev.* **1982**, *82*, 209–222.
(44) Bertho, D.; Laghdir, A.; Jouanin, C. *Phys. Rev. B* **1988**, *38*, 12531–12539.

gap transition which is derived from the lowest energy $\pi-\pi^*$ molecular transition. In bulk polythiophene this absorption band appears near 550 nm. Oxidative doping of polythiophene leads to formation of two types of charges, polarons and bipolarons. Figure 7 presents the simple band picture corresponding to this situation. At low oxidative doping levels, two new electronic levels appear within the gap; these correspond to the polaron (molecular cation radical).

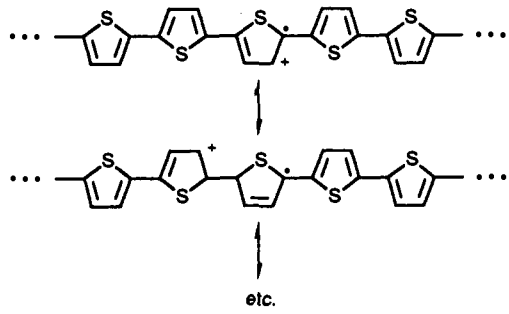

By convention the magnitude of the splitting of the two gap levels is assigned the value $2\hbar\omega_0$. These levels are derived from orbitals near the upper edge of the valence band and the lower edge of the conduction band. The lower level is half occupied so the polaron has spin $^1/_2$ and is EPR active. The presence of the polaron electronic levels in the gap leads to the creation of three new allowed electronic transitions in addition to the band gap transition. Of these, only the intragap transition which connects two discrete orbitals is expected to be sharp (see Figure 7). Theoretical calculations indicate that the intragap transition, $2\hbar\omega_0$ and lowest energy transition $\hbar\omega_1$ should have the largest oscillator strengths.[45,46] To first order for symmetric splitting of the polaron levels about the center of the bands, the energies of the transitions are related by eq 1. We note that for reasonable estimates of

$$\hbar\omega_1 = {}^1/_2(\hbar\omega_g - 2\hbar\omega_0) \quad (1a)$$

$$\hbar\omega_3 = \hbar\omega_1 + 2\hbar\omega_0 \quad (1b)$$

$2\hbar\omega_0$, $\hbar\omega_1$ appears at low energy (less than 5000 cm^{-1}) and $\hbar\omega_3$ is correspondingly close in energy to $\hbar\omega_g$, making experimental observation of either of these transitions difficult under our conditions. The band gap transition $\hbar\omega_g$ is expected to be perturbed only slightly for the polaron compared to undoped oligomer, making it particularly difficult for us to observe as we generally have an excess of undoped oligomer present in our zeolite complexes. The intragap transition of the polaron, $2\hbar\omega_0$, is expected to be readily experimentally observable.

At higher doping levels, the unpaired electron occupying the polythiophene polaron level in the band gap is removed leading to formation of the bipolaron (molecular dication) which is thought to adopt the quinoid structure as shown below.

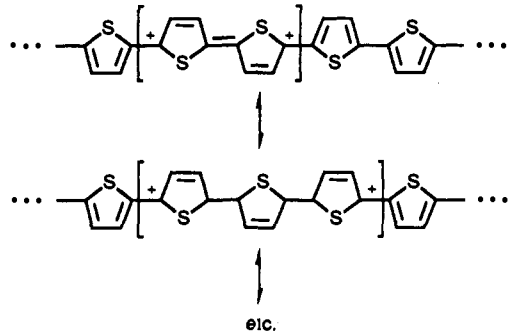

The bipolaron, which is spinless and hence EPR silent, has been demonstrated to be the principal species responsible for charge storage in cationically doped polythiophene.[47] As shown in Figure 7, theory predicts that removal of the second electron leads to a decrease in $2\hbar\omega_0$. The gap levels are now both vacant and the bipolaron thus exhibits only three allowed electronic transitions: $\hbar\omega_g$, $\hbar\omega_1$, and $\hbar\omega_3$. Theoretical calculations predict that the oscillator strength for $\hbar\omega_1$ should be significantly larger than for $\hbar\omega_3$.[45,46] To first order for symmetric splitting of the bipolaron levels about the center of the bands the energies of the transition are related by eq 2. The decreased value of $2\hbar\omega_0$ for the bipolaron

$$\hbar\omega_g = \hbar\omega_1 + \hbar\omega_3 \quad (2)$$

compared to the polaron will lead to a shift of $\hbar\omega_1$ to higher energy making the transition more easily observable. Similarly the position of $\hbar\omega_3$ will be shifted to lower energy away from the band gap transition making it easier to observe as well. As in the case of the polaron, the bipolaron band gap transition, $\hbar\omega_g$, will be similar in energy to that of the neutral polymer and will be difficult to observe in the presence of residual undoped oligomer.

Summarizing the expected spectroscopic properties of the polarons and bipolarons of thiophene oligomers, we expect that in the presence of residual neutral oligomer the polaron (cation radical) will exhibit a single sharp transition in the visible portion of the spectrum. Two additional intragap transitions and the band gap transition of the polaron are expected to be difficult to observe due to either low energy or interfering absorption of the neutral oligomer. The bipolaron will exhibit two transitions, the energies of which sum to the band gap, with the band gap transition obscured by residual neutral. All of these transitions are expected to have energies which depend upon the oligomer chain length.

Determination of Oligomer Chain Lengths and Assignment of Spectra. With this theoretical background in hand, we now turn to the detailed assignment of the optical spectra of the oxidized thiophene oligomers. The first point that must be addressed is the question of chain lengths of the oligomerized products within the zeolite. One approach to establishing the chain length of oligomers formed from the reaction of terthiophene cation radical is to selectively methylate terthiophene to prevent the dimerization/oligomerization from proceeding. Within the straight channels of ZSM-5, there is insufficient free volume for bimolecular reactions in anything other than the terminal α-positions of the thiophene oligomers. Hence, if cation radicals of **3**, **Me-3**, and **Me_2-3** (**$3^{\bullet+}$**, **Me-$3^{\bullet+}$**, and **Me_2-$3^{\bullet+}$**, respectively) are generated in the channels, **Me-$3^{\bullet+}$** is expected only to dimerize to yield hexamer and **Me_2-$3^{\bullet+}$** should yield a stable oxidized product incapable of futher oligomerization.

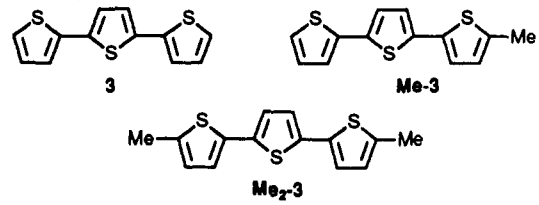

The diffuse reflectance spectra of these compounds included in Na-ZSM-5 (Figures 8 and 9) demonstrate that this is precisely what happens. Turning first to the region near 530 nm, all three terthiophene derivatives exhibit an intense absorption band in this region consistent with oxidation to form the cation radical (polaron). This assignment is readily confirmed from EPR spectra which show a broad slightly structured line at $g = 2.0028$ for **3** and broad bands with poorly resolved hyperfine coupling to the methyl protons for **Me-3** and **Me_2-3** (Figure 3). Unfortunately, these poorly resolved EPR spectra are the rule rather than the exception for cation radicals generated within these zeolites.[1] We have investigated the effect of temperature on the spectra between 4.2 and 410 K and find that there is no major improvement in resolution of the spectra, although there may be slight improvement for the methylated derivatives at the higher temperatures.

(45) Fesser, K.; Bishop, A. R.; Campbell, D. K. *Phys. Rev. B* **1983**, *27*, 4804-4825.

(46) Sum, U.; Fesser, K.; Büttner, H. *Ber. Bunsen-Ges. Phys. Chem.* **1987**, *91*, 957-959.

(47) Chung, T.; Kaufman, J. H.; Heeger, A. J.; Wudl, F. *Phys. Rev. B* **1984**, *30*, 702-710.

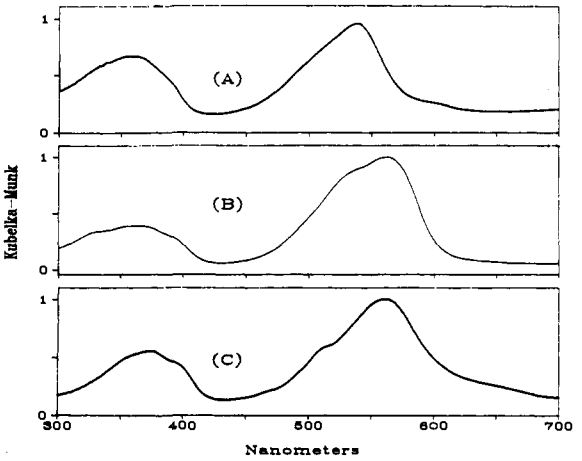

Figure 8. Diffuse reflectance spectra of (A) **3**, (B) **Me-3**, and (C) Me_2-**3** included in Na-ZSM-5 in the region between 300 and 700 nm. The spectra have been normalized to unit absorbance for clarity.

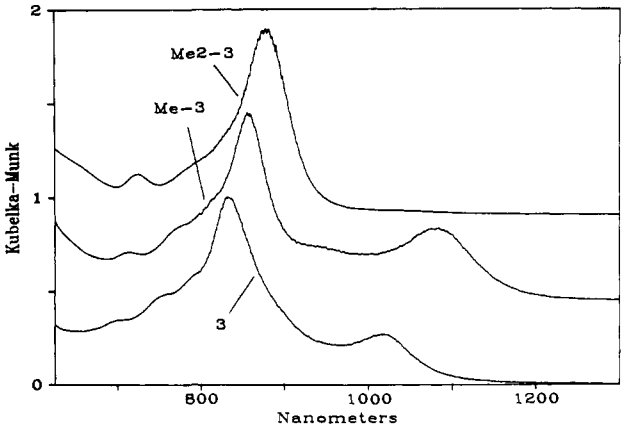

Figure 9. Diffuse reflectance of **3**, **Me-3**, and Me_2-**3** included in Na-ZSM-5 in the region between 625 and 1300 nm (same samples as in Figure 8). The spectra have been normalized to unit absorbance and displaced vertically for clarity.

At this point as the spectra are clearly too poorly structured to yield useful coupling information, we can only note that the appearance significant coupling to the methyl protons for **Me-3**$^{\bullet+}$ and **Me**^{2}-**3**$^{\bullet+}$ is consistent with reports in the literature on the EPR spectra of cation radicals of methylthiophenes generated via γ-irradiation at low temperatures[48,49] and by chemical oxidation in zeolites[28] and in solution.[50]

Turning now to the longer wavelength portion of the spectra in Figure 9, systematic differences with methylation become more apparent. All three complexes show a sharp slightly structured band between 800 and 900 nm with the band shifting to longer wavelength by 300 cm^{-1} per methyl substitution. Note that this band cannot be associated with the initially formed cation radical as it is absent at early reaction times (Figure 2). The fact that this band appears independent of the degree of methylation and that it is absent at early times suggests two possible interpretations. The first is that it is due to oligomerization at the β position to give either **6**-$\alpha\beta$ or **6**-$\beta\beta$ (R = H, Me) and/or their oxidation products. We believe that this is not the correct assignment for several reasons. The spectra of these β-linked dimers have been investigated and found to show minimal conjugation between the two halves of the dimer and hence exhibit spectra resembling simply the sum of the spectra of the two halves of the molecule.[51]

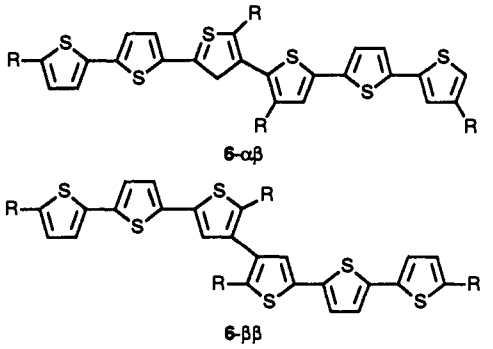

6-$\alpha\beta$

6-$\beta\beta$

This is in contrast to the dramatic red shift in our spectra as compared to **3** or **3**$^{\bullet+}$. We also note that in the case of **Me-3**, β-position dimerization would lead to the formation of six different isomers depending upon the relative disposition of the methyl groups (assuming reaction is only possible at the terminal rings). This would lead to broadening of the spectra in the case of **Me-3** compared to the symmetric species **3** and Me_2-**3** where only one isomer can form. However, the spectra in Figure 9 plainly show both band shapes and widths for all three complexes are nearly identical with only the peak positions affected by methyl substitution.

Steric restrictions in the zeolite channels also make this β-position dimerization improbable, as it would have to occur at the intersection of the straight and zigzag channels between one terthiophene in each of the two channels. Terthiophene, however, is too long (≈19.5 Å as estimated from models) to readily enter the zigzag channels whose straight sections are only ca. 18.0 Å long, effectively making the reaction impossible. We believe the correct assignment of the 800-nm bands is to formation of terthiophene dications (bipolarons). Chemically, this is certainly not unrealistic given both the significant stabilization afforded the dication via the quinoid resonance structure **3**$^{2+}$ and the fact

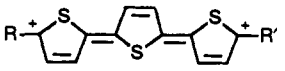

3^{2+}: R = R′ = H
Me-3^{2+}: R = H; R′ = Me
Me_2-**3**$^{2+}$: R = R′ = Me

that **3**$^{2+}$ is strictly analogous to the structure of the bipolaron implicated as the site of charge storage in doped bulk polythiophene. The spin-paired dication, **3**$^{2+}$, is expected to exhibit no EPR signal. Unfortunately we are unable to prepare samples in which only the terthiophene dications are present uncontaminated by the cation radicals, all of which are EPR active. At this point we can only say that no new EPR signals are observed in samples showing the formation of the bipolaron, **3**$^{2+}$, consistent with its assignment as a spin-paired species.

Referring again to Figure 9, we see that in addition to the ~800-nm dication bands present in the spectra of all three derivatives, a second well-resolved band is observed near 1000 nm with an associated vibronic shoulder (spacing ca. 1200 cm^{-1}) in the spectra of **3** and **Me-3**. These bands shift to the red with methylation, but with an apparent sensitivity of 550 cm^{-1} per methyl group, roughly twice that observed for the methyl derivatives of **3**$^{2+}$. These bands are completely absent for the dimethyl derivative Me_2-**3**, immediately suggesting the assignment of these bands to the products of dimerization of **3** and **Me-3** to yield hexamers **6** and Me_2-**6**, respectively. This is consistent with the apparent greater sensitivity of the band position to methylation;

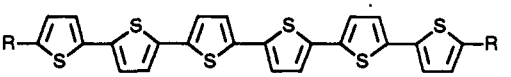

6: R = H
Me_2-**6**: R = Me

the two products differ not by one but by two methyl groups yielding a red shift of 225 cm^{-1} per methyl substitution consistent with the observed shifts for the trimer (300 cm^{-1}/methyl) and

(48) Rao, D.; Symons, M. *J. Chem. Soc., Perkin Tran. II* **1983**, 135-137.
(49) Shiotani, M.; Nagata, Y.; Tasaki, M.; Sohma, J. *J. Phys. Chem.* **1983**, *87*, 1170-1174.
(50) Alberti, A.; Favaretto, L.; Seconi, G.; Pedulli, G. F. *J. Chem. Soc., Perkins Trans. 2* **1990**, 931-935.
(51) Fujimoto, H.; Nagashima, U.; Inokuchi, H.; Seki, K.; Nakahara, H.; Nakayama, J.; Hoshino, M.; Fukuda, K. *J. Chem. Phys.* **1988**, *89*, 1198-1199.

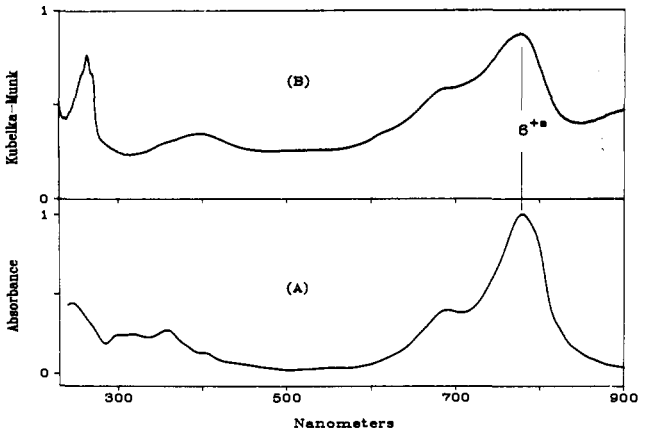

Figure 10. (A) Absorption spectrum of the α-sexithiophene cation radical ($6^{\bullet+}$) in dilute methylene chloride solution. Data taken from ref 6. (B) Diffuse reflectance spectrum of $6^{\bullet+}$ included in Na-β prepared directly from **6** showing only the visible region of the spectrum. The rising tail at longer wavelengths is due to formation of 6^{2+} within the zeolite.

tetramer (225 cm^{-1}/methyl, see below). In the case of Me_2-**3**, the α positions are completely blocked; no dimerization can occur and no long-wavelength band is observed even upon heating of the sample for prolonged periods (see Figure 4). The observed peak positions obviousy cannot be due to the formation of neutral **6** or Me_2-**6** as **6** is a known compound with its absorption maximum at 434 nm in solution.[52] A second possibility is that the long-wavelength absorption band is due to monocations ($6^{\bullet+}$, Me_2-$6^{\bullet+}$). However, this assignment is inconsistent with both the diffuse reflectance spectrum of authentic **6** included in Na-β (Figure 10; due to the low solubility of **6**, we were unable to prepare the Na-ZSM-5 complex directly) and the recently reported solution spectrum[6] of $6^{\bullet+}$, both of which show that the principle absorption maximum for this species appears at 775 nm. The obvious conclusion is that the hexamers are formed as the dications 6^{2+} and Me_2-6^{2+}. This is entirely reasonable particularly given the marked decrease in oxidation potentials of the thiophene oligomers with chain length[52] which makes it likely that for hexamer even the monocation will be readily oxidized. The longer chain oligomers also have an increased chance of encountering the relatively scarce oxidation sites within the zeolite channels. It is not possible with the information which we currently have available to rule out the possibility that further oxidation of the hexamers to trications is occurring; however, we believe that this is unlikely.

A further demonstration of the kinetic orders of the reactions responsible for formation of the bands assigned to 3^{2+} at 833 nm and 6^{2+} at 1019 nm comes from spectra obtained as a function of the initial concentration of **3** in the zeolite. Diffuse reflectance spectra of samples of **3** included in Na-ZSM-5 at loading levels ranging from 0.6% to 0.002% by weight are shown in Figure 11. The spectra have been normalized at 833 nm and the spectra obtained at low loading levels have been carefully base line corrected to remove a weak absorption feature near 800 nm which is due to the zeolite host. These spectra show unambiguously that even at very low concentrations of **3**, the absorption at 833 nm which we have assigned to 3^{2+} is present consistent with formation of this product in a unimolecular reaction. On the other hand, the position of the peak at 1019 nm assigned to 6^{2+} is independent of loading but its intensity decreases relative to that of 3^{2+} as the initial concentration of **3** is decreased. At the lowest loading levels, the only product formed is 3^{2+}, consistent with the product responsible for the 1019-nm peak being formed in a bimolecular reaction. These observations confirm the formation of 6^{2+} via the second-order reaction of two trimers.

The assignment of the 6^{2+} band finds additional support from experiments which employ different oligomeric thiophene precursors. As discussed above, reaction of **2** within Na-ZSM-5 leads to the initial formation of a species assigned as $2^{\bullet+}$. However, $2^{\bullet+}$ is not long lived within the zeolite channels. We find that within a period of a few hours the band at 420 nm due to $2^{\bullet+}$ decreases markedly in intensity and an intense band identical in shape and position to that assigned above to 6^{2+} appears. Weak features consistent with formation of $4^{\bullet+}$ or 4^{2+} appear as well, but it appears that in the presence of excess bithiophene these react rapidly to yield hexamer. Surprisingly, we find that the 6^{2+} formed from **2** does not react further with excess **2** to form higher oligomers, even upon mild heating (60–100 °C). This is the only precursor for which we have observed this type of behavior. We attribute this to the fact that **2** is the only precursor which is short enough to occupy both the straight and zigzag channels in ZSM-5. It appears that the products of oligomerization are forming in both types of channels, in some cases with a single oligomer "going around the corner" between two channels. These oligomers may experience significantly hindered diffusion and as a result are sterically blocked against further reaction.

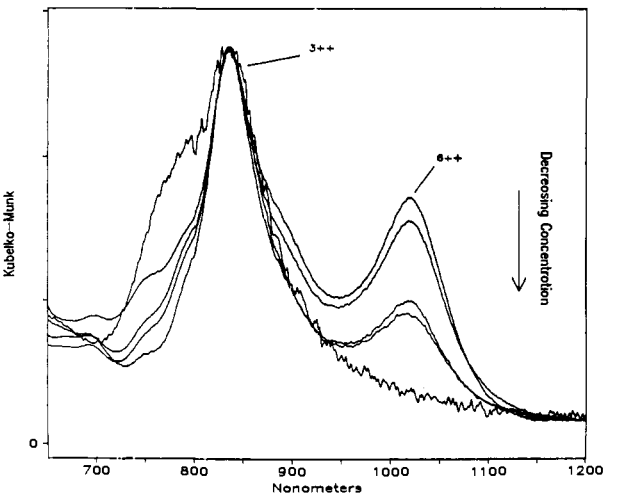

Figure 11. Concentration dependence of the diffuse reflectance spectrum of terthiophene included in Na-ZSM-5. Spectra have been normalized to unit intensity at the 833-nm peak due to 3^{2+}. Terthiophene concentrations for the samples (wt %) are as follows: 0.6%, 0.4%, 0.2%, 0.02%, 0.002%.

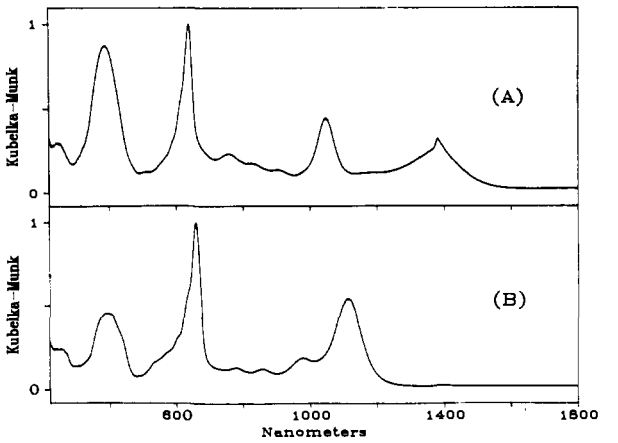

Figure 12. Room temperature diffuse reflectance spectra of (A) quaterthiophene (**4**) included in Na-ZSM-5 and (B) dimethylquaterthiophene (Me_2-**4**) included in Na-ZSM-5. Note the complete absence of the peak near 1400 nm assigned to 8^{2+} in the spectrum of the methylated derivative.

The effect of blocking methyl groups in the case of quaterthiophene (**4**) is shown in Figure 12. Spectra of 4^{2+} and Me_2-4^{2+} are nearly identical except for the consistent 550-cm^{-1} red shift of all peaks observed upon methylation (225 cm^{-1} per methyl substitution) and the complete absence in the Me_2-**4** spectrum of the band centered at 1380 nm which is observed in the spectrum of **4** and which we assign to the lowest bipolaron transition, $\hbar\omega_1$,

(52) Martinez, F.; Voelkel, R.; Naegele, D.; Haarmann, H. *Mol. Cryst. Liq. Cryst.* **1989**, *167*, 227–232.

of the octamer dication, 8^{2+}. The spectra in Figure 12 were acquired under conditions where almost all of the neutral starting material has been converted to dication. We assign the prominent peaks centered near 636 and 1046 nm to the two expected low-energy transitions of the 4^{2+} bipolaron, $\hbar\omega_1$ and $\hbar\omega_3$. Note that the absorption band due to 6^{2+} at 1019 nm is completely absent, as expected since it cannot be formed from a tetrameric precursor. Of the three weak absorption bands appearing between the two bipolaron transitions only the lowest energy one appearing near 980 nm for Me_2-4^{2+} can be assigned to the vibronic structure (1230 cm^{-1}) of the bipolaron. This assignment is confirmed from fluorescence spectra of Me_2-4^{2+} which show good mirror image symmetry to the absorption profile.[53] The origin of the remaining two bands remains uncertain. The relative intensities of these bands to the 4^{2+} bipolaron bands are completely reproducible from sample to sample and we do not believe that they are due to the presence of other reaction products. The most likely explanation is that these bands represent discrete transitions from lower energy molecular orbitals within the valence band to the lower bipolaron level within the gap, pointing out the danger of relying too heavily upon the band picture description for these short-chain oligomers. A similar feature is observed in the spectrum of Me_2-3^{2+} as a single weak band near 720 nm. Further experiments aimed at clarifying the assignments for these weak bands are in progress.

Returning to the data presented in Figure 5 for the oligomerization of **3** in Na-ZSM-5, the results are now directly interpretable. The band which is decreasiing in intensity at 350 nm is due to neutral **3** which is reactiing to form cations and or higher oligomers. The band which is disappearing at 530 nm is due to reaction of $3^{\bullet+}$ to form either higher oligomers or dications, 3^{2+}. The bands at 600 and 1019 nm which are disappearing are due to the 6^{2+}. And finally, we assign the two new bands at 761 and 1480 nm to formation of the next higher oligomer, which must be due either to reaction of hexamer with trimer to yield 9-mer, presumably as 9^{2+}, or to dimerization of hexamers to yield 12-mer again presumably as 12^{2+}. Given the relatively low concentration of oxidation sites within the zeolite (only ≈0.1% of the included monomers can be oxidized in fully loaded zeolite[1]), we know that there is always a large excess of neutral present in the zeolite and we prefer the assignment of the bands at 761 and 1480 nm to 9^{2+} resulting from reaction of 6^{2+} with **3**. While the 761-nm band is close to the position expected for the polaron transition, $2\hbar\omega_0$ of $+6^{\bullet+}$ (775 nm), comparison of many spectra shows that the observed 14-nm shift is reproducible. However, it is likely that $6^{\bullet+}$ contributes to the peak at ≈770 nm in the diffuse reflectance spectra of Figure 5. In fact, the difference spectra clearly show that this peak is shifting to shorter wavelength with reaction time, indicating that while 9^{2+} is forming $6^{\bullet+}$ is also present. The absorption band due to 3^{2+} is not detectable under the conditions of this experiment apparently because its concentration is low and its position is close to the strong bands due to 9^{2+} and $6^{\bullet+}$.

The band shapes of the bipolaron spectra of the thiophene oligomers are noteworthy for the well-resolved vibronic structure which is routinely observed. The spectra typically show vibronic shoulders, with spacings between 1100 and 1300 cm^{-1} for the longer chain bipolarons. To our knowledge, this structure has not been observed for bulk polymer samples, presumably due to the presence of a distribution of chain lengths which leads to inhomogeneous broadening of the spectra. The vibronic spacings are consistent with the observation that doped polythiophene exhibits four strong doping dependent IR transitions at 1330, 1200, 1120, and 1030 cm^{-1}.[54] The observation of vibronic structure appears to be diagnostic for bipolarons; polaron spectra do not exhibit well-resolved vibronic structure in either absorption or emission spectra, although there is evidence for a poorly resolved ≈1700-cm^{-1} vibronic shoulder in spectra of $3^{\bullet+}$.[53] Similar 1100–1300-cm^{-1} vibronic spacings are observed for the bipolarons of the methylated oligomers where we also have evidence for the presence of a second lower energy mode (≈700 cm^{-1})[53] which is close to the value reported for the α–α' interring carbon–carbon stretch in doped polythiophene.[55]

Table I. Electronic Absorption Band Positions for Oligomeric Thiophenes ($2 \le n \le 9$) Included in Na-ZSM-5[a]

oligomer chain length	$\hbar\omega_g$ (neutral)	$2\hbar\omega_0$ (polaron)	$\hbar\omega_3$ (bipolaron)	$\hbar\omega_1$ (bipolaron)
2	300	407		
3	354	522		833
4	390	614	636	1046
6	434	775	600	1019
8			661	1383
9			761	1450

[a] The positions cited are the peak maxima in nanometers for the 0–0 vibronic transitions observed in room temperature diffuse reflectance spectra. Higher energy vibronic peaks are not included in the table. Literature values of the absorption band maxima for the neutral oligomers in solution are included for comparison.[52]

Correlations of Spectroscopic Energies with Oligomer Chain Lengths. In the preceding sections, we have discussed the assignment of the optical spectra of the thiophene oligomers and their corresponding polarons and bipolarons within Na-ZSM-5 and Na-β zeolites. Table I summarizes these results for thiophenes with chain lengths between 2 and 9. In all cases, we have attempted to assign the $2\hbar\omega_0$ transitions for the polarons, and the $\hbar\omega_1$ and $\hbar\omega_3$ transitions for the bipolarons, although due to the complex nature of the spectra some bands have not been located. We also find no evidence of polarons in spectra of oligomers with chain lengths longer than 6. This is consistent both with the decreased oxidation potentials of the longer oligomers and with the difficulty in locating the polaron transitions in bulk polymer (see below). In comparing spectroscopic results for the doped oligomers it is important to note that we are comparing species whose doping levels are *constant* if one considers the number of defects per oligomer chain (i.e. either one polaron or bipolaron). In a sense our results are obtained at the limit of zero doping.

The peak positions for the neutral oligomers, polarons, and bipolarons all vary in a systematic way with inverse chain length as shown in Figure 13. This dependence appears to be a manifestation of the well-known reciprocal rule for polymers[56–58] which has been observed previously both experimentally[52] and theoretically[59] for the band-gap absorption of neutral thiophene oligomers. To our knowledge, this is the first experimental observation of this phenomenon for polarons and bipolarons of conducting polymers. Detailed analyses of these dependences provide useful predictions of properties of bulk doped polythiophene as discussed below.

Polarons. There are a number of predictions of the simple band model which can be considered in light of the results summarized in Figure 13. Turning first to the transition assigned to $2\hbar\omega_0$ for the polaron, and assuming that the levels within the gap are split symmetrically about the center, the positions of the two unobserved transitions, $\hbar\omega_1$ and $\hbar\omega_3$, can be calculated (eq 1). As expected, for $\hbar\omega_1$ the estimated position lies at very low energy varying from 4600 cm^{-1} (2170 nm) for $3^{\bullet+}$ to 4900 cm^{-1} (2040 nm) for $9^{\bullet+}$. This is outside our experimental range and consistent with our inability to find any low-energy bands associated with the presence of the thiophene polarons. The other polaron transition, $\hbar\omega_3$, which must lie intermediate in energy between $\hbar\omega_g$ and $2\hbar\omega_0$, also remains unobserved. This is consistent with theoretical calculations which predict this transition should have low oscillator strength.[45,46]

(53) Caspar, J. V.; Ramamurthy, V.; Corbin, D. R. To be published.
(54) Hotta, S.; Shimotsuma, W.; Taketani, M. *Synth. Met.* **1984**, *10*, 85-94.
(55) Tourillon, G. In *Handbook of Conducting Polymers*; Skothem, T. A., Ed.; Marcel Dekker: New York, 1986; Vol. I, pp 293-350.
(56) Duke, C. B.; Paton, A.; Salaneck, W. R. *Mol. Cryst. Liq. Cryst.* **1982**, *83*, 177.
(57) Diaz, A. F.; Crowley, J.; Baryon, J.; Gardini, G. P.; Torrance, J. B. *J. Electroanal. Chem.* **1981**, *121*, 355.
(58) Brêdas, J. L.; Chance, R. R.; Silbey, R. *Mol. Cryst. Liq. Cryst.* **1981**, *77*, 319.
(59) Lahti, P. M.; Obrzut, J.; Karasz, F. E. *Macromolecules* **1987**, *20*, 2023-2026.

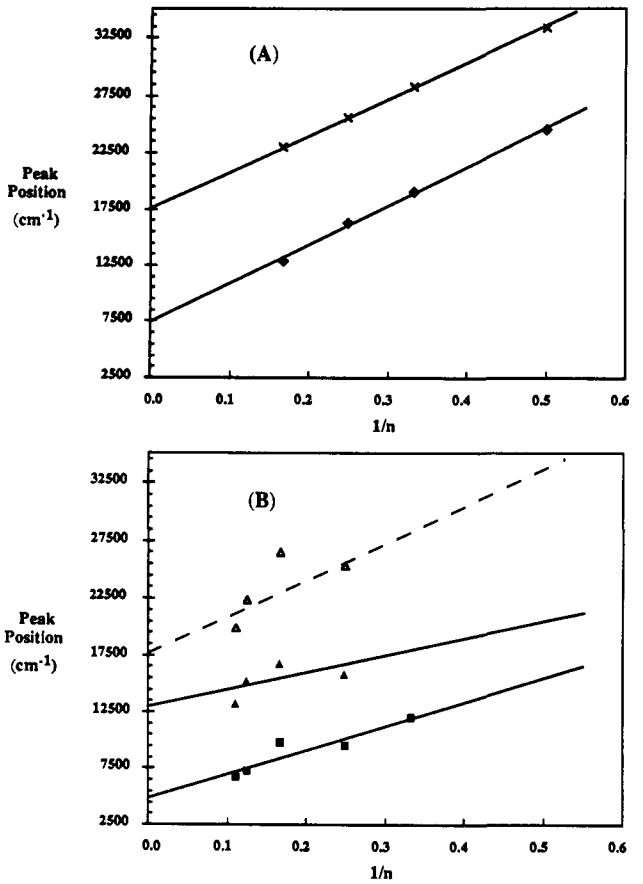

Figure 13. Plot of the dependence of electronic absorption band energies for oligomeric thiophenes as a function of the inverse chain length, n^{-1}; (X) $\hbar\omega_g$ for neutral oligomers in solution; (♦) $2\hbar\omega_0$ for polarons included in Na-ZSM-5; (■) $\hbar\omega_1$ for bipolarons included in Na-ZSM-5; (▲) $\hbar\omega_3$ for bipolarons included in Na-ZSM-5; (△) $\hbar\omega_1 + \hbar\omega_3$ for bipolarons included in ZSM-5-3. The dashed line in (B) is the least-squares line for the neutrals in (A).

It is useful to consider the extrapolation of the data in Figure 13 to the intercept, $n^{-1} = 0$, which corresponds to the limiting case of infinite chain length polymer. It has been shown previously that extrapolations of this type yield good estimates for the band gap of neutral polythiophene;[59] the data in Figure 13 yields a value of $\hbar\omega_g = 17\,400 \pm 200$ cm^{-1} in excellent agreement with the literature value of 16 100 cm^{-1}.[60] We are now in a position to carry out the same extrapolation procedure for the transitions due to the polaron and bipolaron. Obviously, if the zeolite-encapsulated doped oligomers are going to represent useful models of polythiophene, this extrapolation must yield transition energies which are in reasonable agreement with results obtained by direct measurement of doped polymer. Our data extrapolate to a value of 7400 ± 430 cm^{-1} (1350 nm) for $2\hbar\omega_0$ for the polaron in bulk polythiophene. The energy of this transition has been estimated experimentally from absorption spectroscopy at low polythiophene doping levels to be near 10000 cm^{-1} (1000 nm)[61,62] although this assignment is controversial.[63,64] While the discrepancy with our prediction is not large, our data do not appear to support this assignment. It is interesting to note that in the case of polypyrrole, which is closely related to polythiophene both structurally and electronically, the $2\hbar\omega_0$ polaron transition has been unambiguously assigned to a band at 9700 cm^{-1}.[65] If we scale this energy by the ratio of band gaps of the two neutral polymers (polythiphene = 17 700 cm^{-1}, polypyrrole = 24 200 cm^{-1}, ratio = 0.73), $2\hbar\omega_0$ for polythiophene is predicted to be 7100 cm^{-1}, in excellent agreement with the prediction from our data.

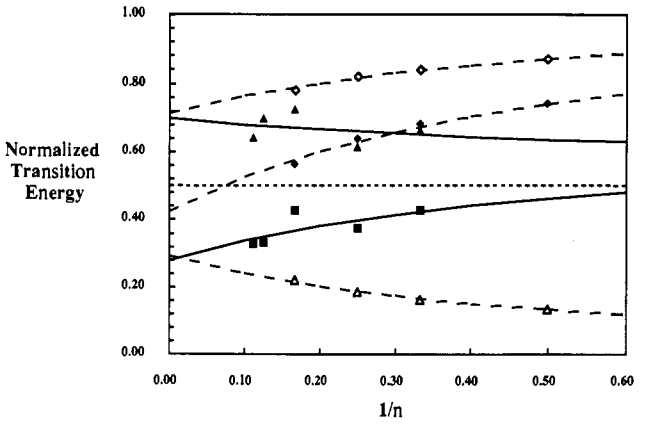

Figure 14. Plot of the dependence of the normalized transition energies for the polaron and bipolaron transitions of the oligomeric thiophenes included in Na-ZSM-5 as a function of the inverse chain length (see the text for details of the calculation): (♦) $2\hbar\omega_0$, polaron; (△) $\hbar\omega_1$, polaron, calculated with eq 1a; (◇) $\hbar\omega_3$, polaron, calculated with eqs 1a and 1b; (▲) $\hbar\omega_3$, bipolaron; (■) $\hbar\omega_1$, bipolaron.

Bipolarons. Turning to the bipolaron and again assuming that the gap levels are split symmetrically, the simple band model predicts the two bipolaron transition energies should sum to the band gap. As shown in Figure 13, this prediction is consistent with the data; the experimentally determined sums are in good agreement with the band gap transitions of the neutral oligomers. Repeating the extrapolation to infinite polymer described above, we can now predict the positions of the $\hbar\omega_1$ and $\hbar\omega_3$ bipolaron absorption bands bulk doped polythiophene. Our data yield values of 12900 ± 2400 cm^{-1} (775 nm) for $\hbar\omega_3$ and 5000 ± 1050 cm^{-1} (2000 nm) for $\hbar\omega_1$, in remarkable agreement with the experimental values of 12100 cm^{-1} ($\hbar\omega_3$) and 5200 cm^{-1} ($\hbar\omega_1$).[41,47] This clearly demonstrates that the zeolite encapsulated thiophene oligomers are excellent short-chain models for doped polythiophene.

It is particularly interesting to consider the implications of these results upon the proposed structure of polythiophene. As prepared, polythiophene is amorphous and as a result the question of the molecular conformation of the thiophene chains remains unresolved. Two limiting structures have been proposed for the polymer, a linear arrangement with sulfurs arranged in a trans configuration between adjacent monomer units and a helical structure with the sulfurs all cis.[55] In the context of our experiments, only the linear structure is small enough sterically to fit into the channels of the zeolite hosts. Given the remarkable agreement of the predicted bipolaron absorption band positions from the zeolite-encapsulated oligomers with the results for bulk polymer, our data are clearly consistent with a linear structure for bulk polythiophene, but the data do not necessarily rule out the helical structure.

Normalization of Transition Energies to Constant Band Gap. The systematic dependence of the polaron and bipolaron band positions on inverse chain length is gratifying and allows the prediction of band positions in bulk polythiophene. Unfortunately, as so many parameters are changing throughout the oligomer series, it is not readily apparent how this chain length dependence translates into an understanding of the sensitivity of the positions of the polaron and bipolaron levels in the band gap to chain length. In particular, $\hbar\omega_g$ is decreasing dramatically as chain length increases (see Figure 7). To demonstrate the trends in the polaron and bipolaron positions within the gap as a function of chain length, we have elected to normalize the observed band positions to constant band gap by dividing the transition energies by $\hbar\omega_g$.

(60) Kobayashi, M.; Chen, J.; Chung, T.; Moraes, F.; Heeger, A. J.; Wudl, F. *Synth. Met.* **1984**, *9*, 77.
(61) Kaneto, K.; Hayashi, S.; Ura, S.; Yoshino, K. *J. Phys. Soc. Jpn.* **1985**, *54*, 1146.
(62) Kaneto, K.; Kohno, Y.; Yoshino, K. *Mol. Cryst. Liq. Cryst.* **1985**, *118*, 217-220.
(63) Moraes, F.; Schaffer, H.; Kobayashi, M.; Heeger, A. J.; Wudl, F. *Phys. Rev. B* **1984**, *30*, 2948.
(64) Vardeny, Z.; Ehrenfreund, E.; Brafman, O.; Nowak, M.; Schaffer, H.; Heeger, A. J.; Wudl, F. *Phys. Rev. Lett.* **1986**, *56*, 671-674.
(65) Kaufman, K. H.; Colaneri, N.; Scott, J. C.; Kanazawa, K. K. *Mol. Cryst. Liq. Cryst.* **1985**, *118*, 171-177.

In order to avoid problems due to broad overlapping transitions in the region of the band gap in the zeolite-included oligomers, we have chosen to use values of $\hbar\omega_g$ taken from solution spectra.[52] Furthermore, as reliable values do not appear to be available for chain lengths longer than 6, we have elected to obtain estimates of $\hbar\omega_g$ for higher chain lengths via extrapolation using the n^{-1} dependence. Figure 14 presents the results of this manipulation for the polaron and bipolaron transitions of the thiophene oligomers. In the figure, the solid lines are just the least-squares lines from Figure 13 which now appear as curves as a result of the $\hbar\omega_g$ normalization. The effect of chain length increase upon the energy of the bipolaron levels is now much clearer; as chain length increases, the two bipolaron levels are splitting neary symmetrically about the band center, just as expected from simple theory. At a more detailed level, we note that the splitting is actually slightly asymmetric with the upper bipolaron level on average destabilized by about 5% more than the lower bipolaron level is stabilized, consistent with expectations from simple first-order perturbation theory.

Figure 14 also includes the predicted positions of the polaron levels which are calculated from eq 1 assuming symmetric splitting of the levels. The striking aspect of the calculated positions of these levels lies in the extrapolation to the bulk polymer limit. The extrapolated normalized positions of the lower polaron and bipolaron levels are calculated to be 0.29 ± 0.02 and 0.28 ± 0.06, respectively. In absolute energies (calculated neglecting doping induced changes in the band gap), we estimate that the polaron lies 5150 cm^{-1} above and the bipolaron 4950 cm^{-1} above the valence band and hence that the bipolaron is only about 200 cm^{-1} lower in energy than the polaron in doped polythiophene. If the theoretical prediction that $\hbar\omega_g$ increases in order neutral < polaron < bipolaron is correct, then our estimate of the energy difference between the polaron and bipolaron represents a lower limit. We emphasize that our results are determined in the limit of zero doping (one defect per chain) and may not necessarily reflect the energetics at higher doping levels.

This estimate of the relative energies of the polaron and bipolaron has direct implications for the mechanism of interchain electron hopping in doped polythiophene, a process which plays an important role in the bulk electronic conductivity of the polymer. Our results suggest that given the similar energies of these two levels, the transfer of bipolarons between chains need not necessarily occur in a single concerted step. Rather, it appears energetically feasible to split the bipolaron into two polarons which could then independently transfer between polymer chains followed by recombination to reform the bipolaron.

Conclusion

In this paper, we have demonstrated that pentasil zeolites can be used as supporting matrices in which short-chain oligomers of polythiophene can be prepared, doped to the conducting state, stabilized, and spectroscopically characterized. For the first time, the evolution of the electronic structure of doped polythiophene from monomer to polymer has been observed directly for chain lengths between two and nine. Plots of the electronic absorption band energies for the polarons and bipolarons were found to be linear functions of inverse chain length. These results were extrapolated to infinite chain length to predict the positions of the electronic transitions of bulk polythiophene. In addition, we have demonstrated experimentally that the energies of the lowest polaron and bipolaron levels of doped polythiophene are remarkably similar, suggesting that transient formation of polarons from bipolarons could play a role in interchain charge hopping in this material.

We are continuing our work in this area along a number of lines. In particular, the Franck–Condon analysis of low-temperature absorption and fluorescence spectra of the excited states of the doped thiophene oligomers is providing direct evidence about structural distortions of the polaron and bipolaron. Investigation of the vibrational spectra of the doped oligomers is in progress. We are also investigating the temperature dependence of the thiophene oligomerization in order to further elucidate the kinetics and mechanism of the reaction within the zeolite channels. We expect to expand the range of polymers under investigation. In particular the oxidation of short-chain polyenes as models for polyacetylene has already been demonstrated[1] and we are in the process of extending these studies to longer chain substrates.

Acknowledgment. We thank D. Sanderson, A. Pittman, and P. Hollins for able technical assistance.

Registry No. **2**, 56902-08-0; **3**, 111744-23-1; **4**, 127473-73-8; **6**, 127473-75-0; **8**, 130468-58-5; **9**, 130468-59-6.